

# Transition metal based functional coatings: Effect of the choice of metal element

**Jiri Houska**, P. Mares, J. Kohout,  
R. Cerstvy, S. Zuzjakova, J. Vlcek

*Department of Physics and NTIS - European Centre of Excellence,  
University of West Bohemia, Czech Republic*



DEPARTMENT  
OF PHYSICS



## Acknowledgment

Grant Agency of the Czech Republic through Project No. 15-00859Y



## Outline (materials discussed)

- MBCN [ *J. Houska et al., Thin Solid Films 586, 22 (2015)* ]
- reasons for Si incorporation
- MSiBCN [ *J. Houska et al., Thin Solid Films 616, 359 (2016)* ]

## Motivation

- Combination of theoretical (calculated) and experimental data
- Capture the differences resulting from the M (Ti, Zr, Hf) choice
  - same theoretical and experimental techniques
  - same (calculations) / similar (experiment) M/B/C/N ratios
  - similar (low) compressive stress



## Motivation for M(Si)BCN (M = Ti, Zr, Hf)

hard and wear resistant  
cubic **MN** (e.g. TiN):

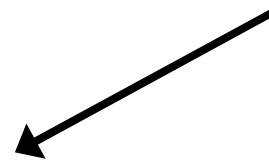
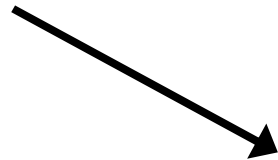


superhard **MN-based  
nanocomposites**  
(e.g. nc-TiN/a-Si<sub>3</sub>N<sub>4</sub>)

**B incorporation** into  
amorphous SiCN



oxidation resistance  
(1500°C) of hard transparent  
amorphous **SiBCN**



Nanostructure design of M(Si)BCN: nc-M(B,C,N)/a-(Si)BCN

Capture differences resulting from M choice

## Elemental composition choice

- 1) at this stage focus on MBCN (Si in second half of the presentation)
- 2) B/C ratio given by  $B_4C$  sputer target

3) not just nanocrystalline  
M(B,C,N) but  
nc-M(B,C,N)/a-BCN



M content  $\ll$  50 at. %

4) not hexagonal  $MB_2$ -based  
crystals but cubic  
MN-based crystals



M/B ratio  $\ll$  2

Compositions around  $M_{41}B_{30}C_8N_{20}$   
(except series with varied N content)



## Experimental methodology

Reminder of the aim: thin films around  $M_{41}B_{30}C_8N_{20}$

$M_{45}(B_4C)_{55}$  sputter target (M = Ti, Zr, Hf)

### DC pulsed magnetron sputtering

- repetition frequency 10 kHz, duty cycle 85%  
( $\Rightarrow$  voltage pulse length  $85 \mu s < t_{krit} = \epsilon_0 \epsilon_r E_{br} / J_{it}$ )
- substrate (Si, glass) temperature 450 °C
- substrates on floating potential around -40V

5%  $N_2$  + 95% Ar plasma (except series with varied N content)

### Bombardement of floating substrates

- by  $Ar^+$  ions (overshoot voltage after switching off each pulse)
- by Ar neutrals reflected from sputter target (depends on M choice)



## Adaptive discharge pressure at M = Ti, Zr, Hf

Ar reflected from target  $\Rightarrow$  compressive stress in growing films

**Fixed pressure** (0.5 Pa), assume elastic head-on collisions of Ar<sup>+</sup> with M target, calculate energy of reflected Ar

M = Ti  $\Rightarrow (m_M - m_{Ar})^2 / (m_M + m_{Ar})^2 = 0.01 \Rightarrow$  low (or tensile) stress

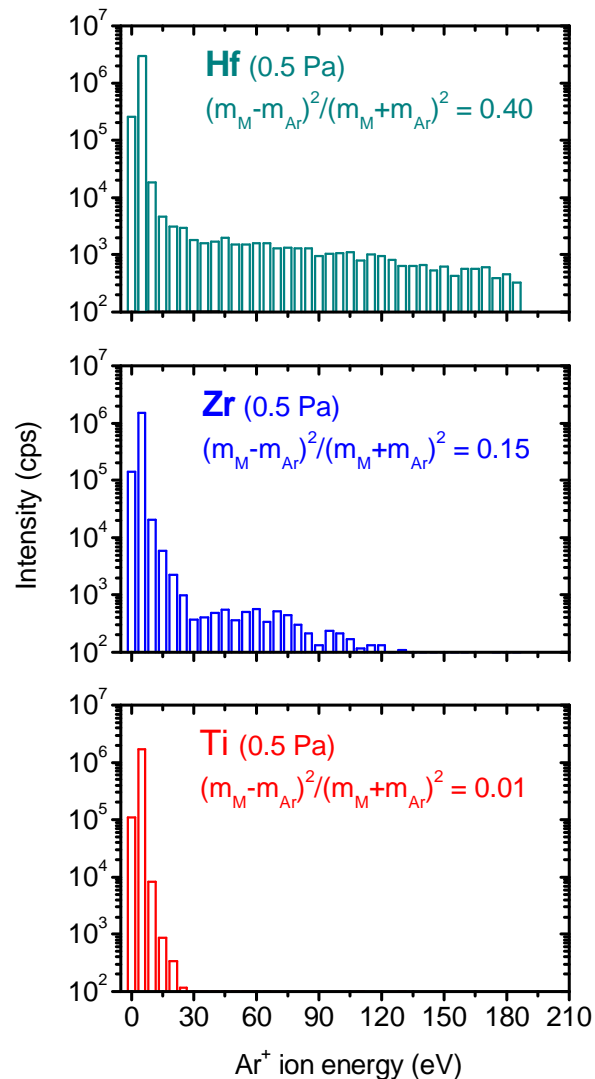
M = Zr  $\Rightarrow (m_M - m_{Ar})^2 / (m_M + m_{Ar})^2 = 0.15 \Rightarrow$  medium stress

M = Hf  $\Rightarrow (m_M - m_{Ar})^2 / (m_M + m_{Ar})^2 = 0.40 \Rightarrow$  high stress

(Monte Carlo simulations: same trend)

(Mass spectroscopy: same trend)

## Adaptive discharge pressure at M = Ti, Zr, Hf



⇒ compressive stress in growing films

, assume elastic head-on collisions  
 calculate energy of reflected Ar

$(m_M - m_{Ar})^2 = 0.01 \Rightarrow$  low (or tensile) stress

$(m_M - m_{Ar})^2 = 0.15 \Rightarrow$  medium stress

$(m_M - m_{Ar})^2 = 0.40 \Rightarrow$  high stress

∴ same trend)

the trend)

## Adaptive discharge pressure at M = Ti, Zr, Hf

Ar reflected from target  $\Rightarrow$  compressive stress in growing films

**Fixed pressure** (0.5 Pa), assume elastic head-on collisions of Ar<sup>+</sup> with M target, calculate energy of reflected Ar

M = Ti  $\Rightarrow (m_M - m_{Ar})^2 / (m_M + m_{Ar})^2 = 0.01 \Rightarrow$  low (or tensile) stress

M = Zr  $\Rightarrow (m_M - m_{Ar})^2 / (m_M + m_{Ar})^2 = 0.15 \Rightarrow$  medium stress

M = Hf  $\Rightarrow (m_M - m_{Ar})^2 / (m_M + m_{Ar})^2 = 0.40 \Rightarrow$  high stress

**Varied pressure** in order to slow energetic Ar down by collisions

M = Ti  $\Rightarrow (m_M - m_{Ar})^2 / (m_M + m_{Ar})^2 = 0.01 \Rightarrow$  **low stress at 0.35 Pa**

M = Zr  $\Rightarrow (m_M - m_{Ar})^2 / (m_M + m_{Ar})^2 = 0.15 \Rightarrow$  **low stress at 0.5 Pa**

M = Hf  $\Rightarrow (m_M - m_{Ar})^2 / (m_M + m_{Ar})^2 = 0.40 \Rightarrow$  **low stress at 1.7 Pa**

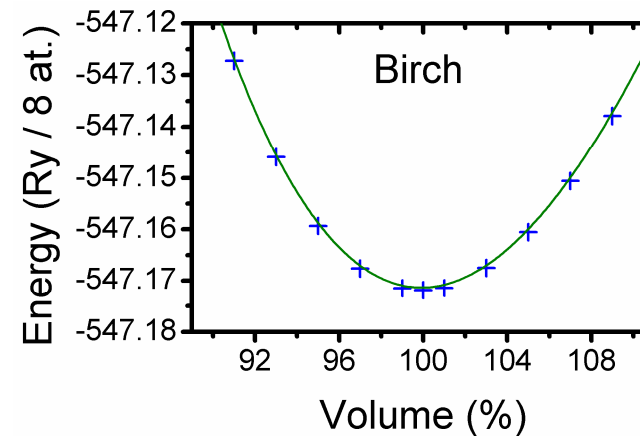
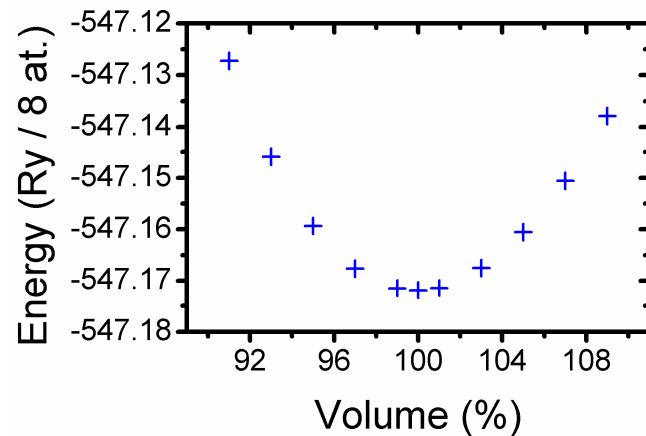


## Support of experiment by ab-initio calculations

Motivation: calculate formation energies of fcc-MB<sub>x</sub>C<sub>y</sub>N<sub>1-x-y</sub>

- with respect to fcc-MN + fcc-MC + MB<sub>2</sub> + M  
(stable constituent phases)
- with respect to fcc-MN + fcc-MC + fcc-MB  
(less stable but isostructural)

For each phase: calculate energy ( $E_0$ ) from  $E(V)$  dependence



Birch eq. of state:  $E = E_0 + 9/8 B_0 V_0 ([V_0/V]^{2/3} - 1)^2 + 9/16 B_0 (B' - 4) V_0 ([V_0/V]^{2/3} - 1)^3$



## Theoretical methodology

### DFT as implemented in PWscf code

- Atom cores + inner electron shells: Vanderbilt-type ultrasoft pseudopotentials
- Valence electrons: plane wave basis, energy cutoff of 30 Ry
- Exchange-correlation term: Perdew-Burke-Ernzerhof functional
- Brillouin zone sampling  $12 \times 12 \times 12$  k-points for 8 atoms

### Periodical simulation cell

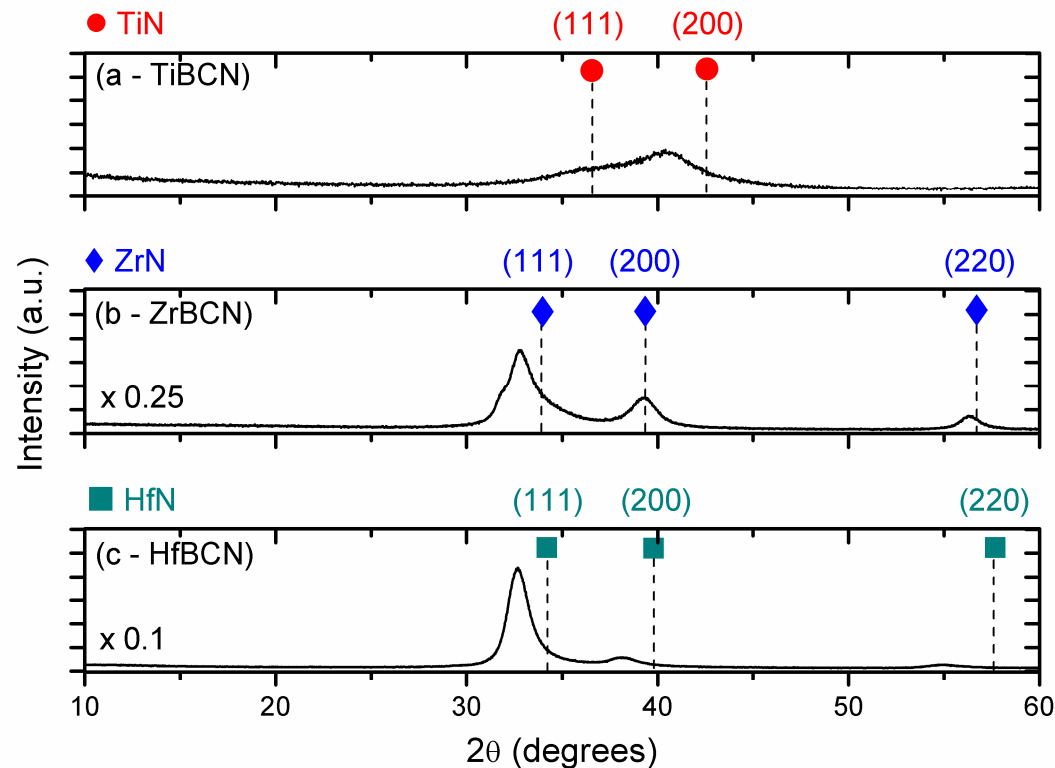
- 8 atoms (uniform distribution of atoms in fcc- $\text{MB}_x\text{C}_y\text{N}_{1-x-y}$ )
- 48 atoms (cross-check using quasirandom distribution)

## Effect of M choice on structure of $M_{41}B_{30}C_8N_{20}$

M = Ti: X-ray amorphous

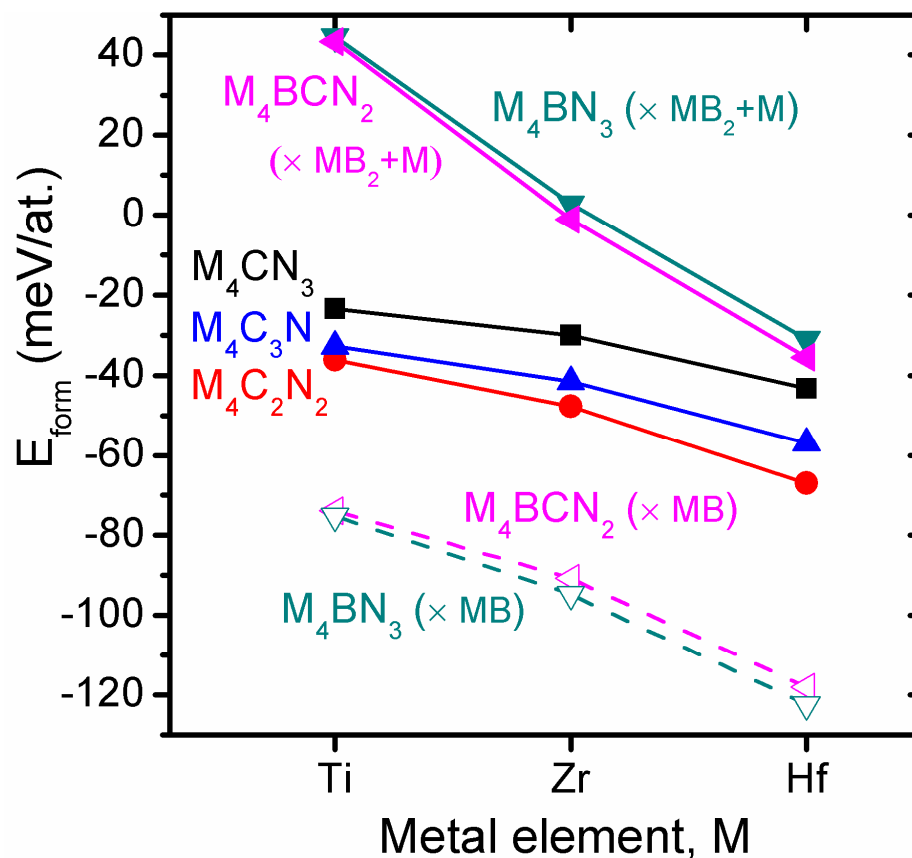
M = Zr: ZrN-like crystals, shift of 111 peak towards e.g. ZrB

M = Hf: HfN-like crystals, shift of all peaks towards e.g. HfB



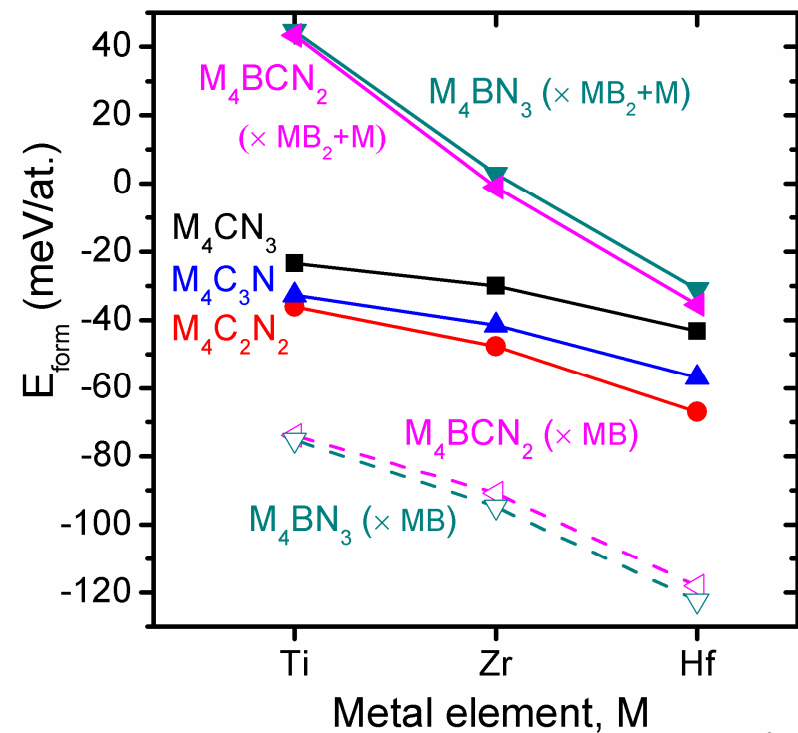
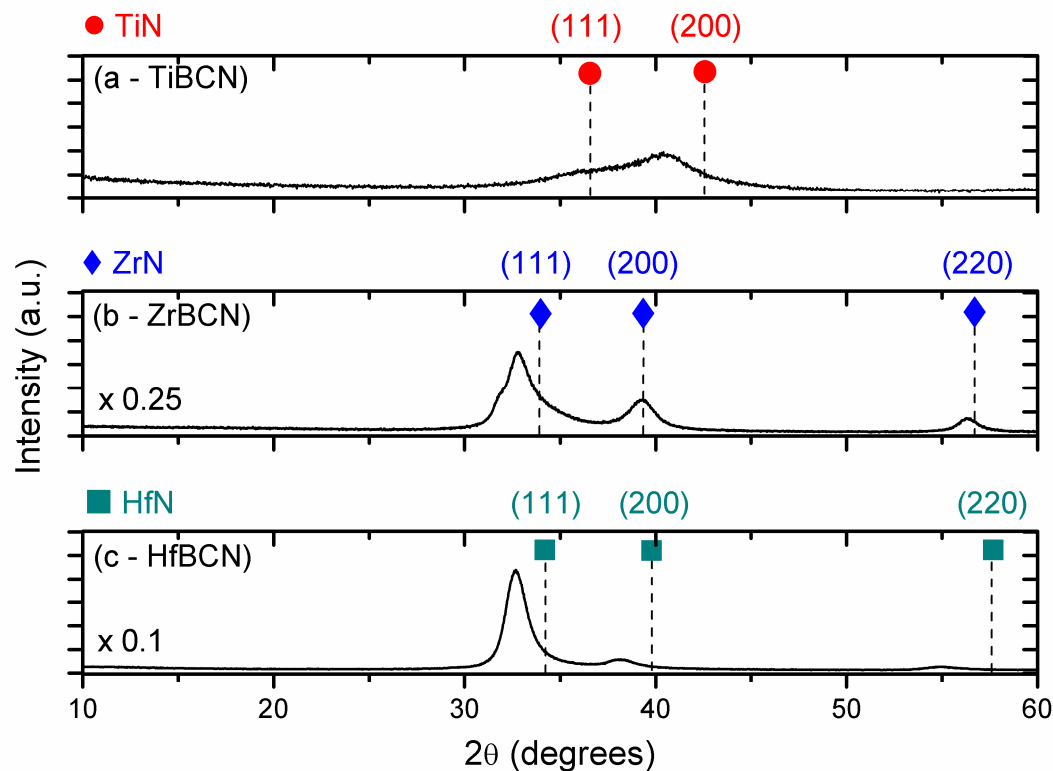
## Effect of M choice on structure of $M_{41}B_{30}C_8N_{20}$

Transition from M = Ti through Zr to Hf  $\Rightarrow$   
decreasing formation energy ( $\Rightarrow$  more likely formation)  
of all  $MB_xC_yN_{1-x-y}$  solid solutions considered



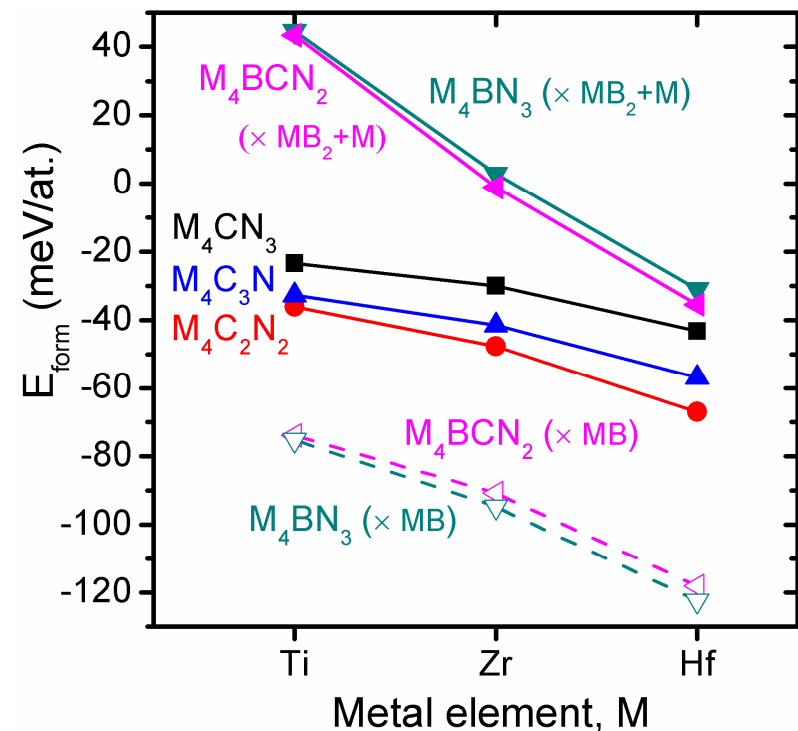
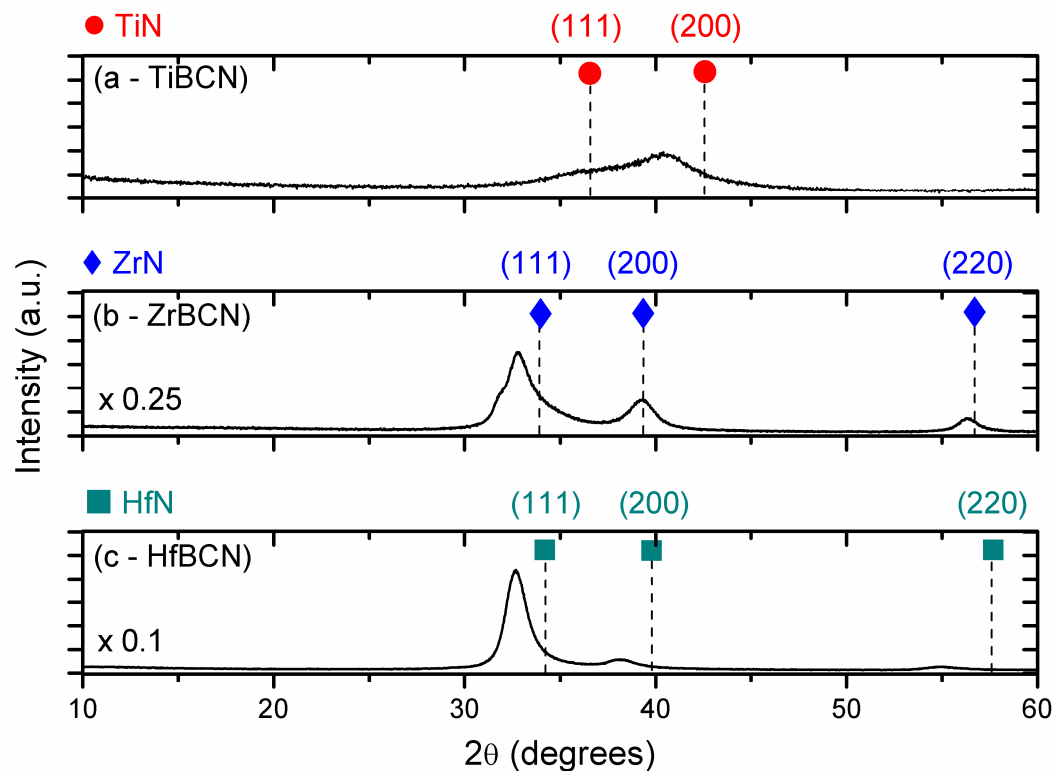
## M = Ti: x-ray amorphous

- largely positive  $E_{\text{form}}$  of all B-containing crystals
- formation of B-free  $\text{TiC}_y\text{N}_{1-y}$  is thermodynamically OK, but kinetically difficult (low C+N content; low E of bombarding Ar)



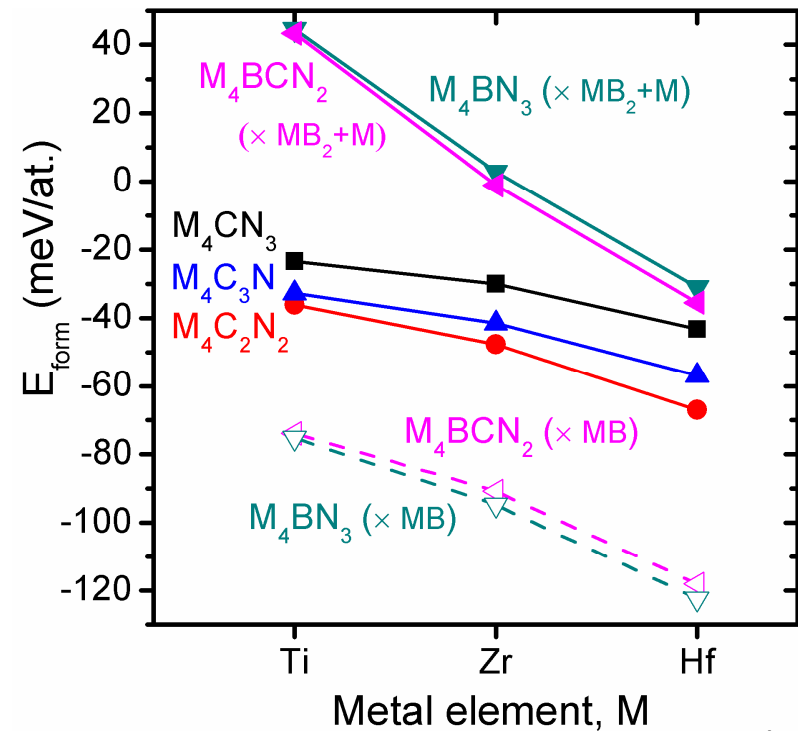
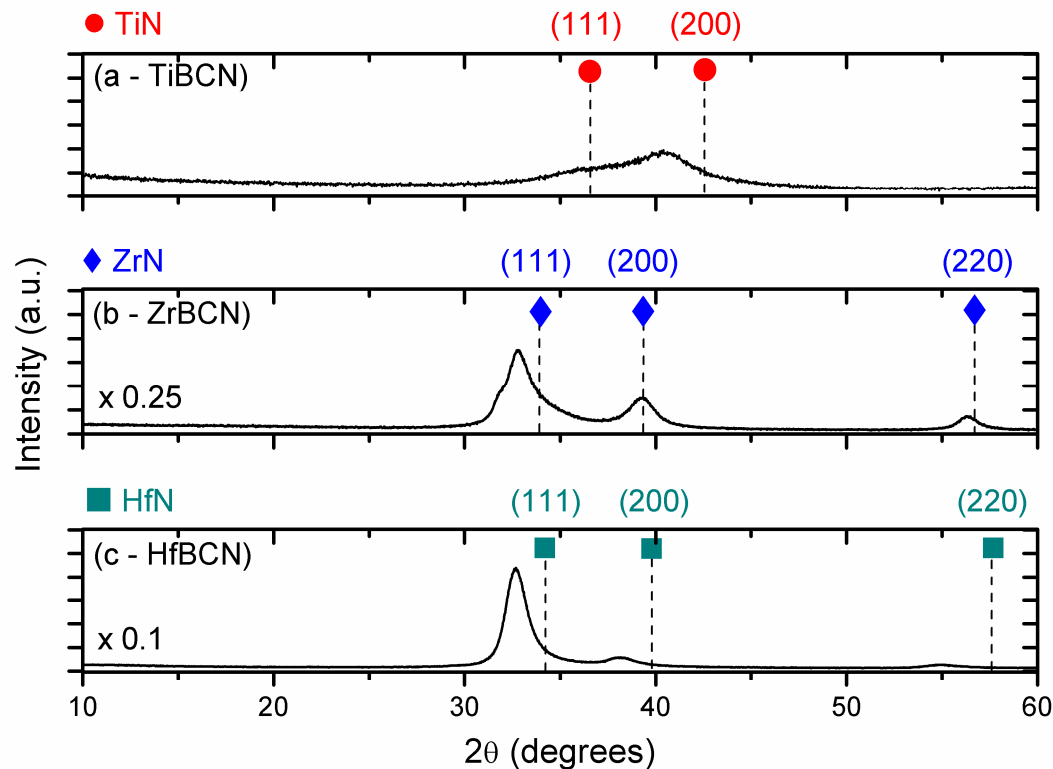
## M = Zr: ZrN-like crystals, shift of 111 peak towards ZrB

- at least 111 crystals are fcc- $\text{ZrB}_x\text{C}_y\text{N}_{1-x-y}$  solid solutions; explained by  $E_{\text{form}} \sim 0$  for  $\text{ZrB}_{0.25}\text{C}_{0.25}\text{N}_{0.50}$  or  $\text{ZrB}_{0.25}\text{N}_{0.75}$
- consistent lattice constant differences from pure ZrN (3.1% from XRD, e.g. 2.1% calculated for  $\text{ZrB}_{0.25}\text{C}_{0.25}\text{N}_{0.50}$ )



## M = Hf: HfN-like crystals, shift of all peaks towards HfB

- all crystals are fcc-HfB<sub>x</sub>C<sub>y</sub>N<sub>1-x-y</sub> solid solutions; explained by even lower  $E_{\text{form}}$  values (compared to M = Zr)
- more pronounced texture/crystallinity (XRD peaks scaled down) and 111 preference (compared to M = Zr)





## Effect of M choice on structure of $M_{41}B_{30}C_8N_{20}$

Summary of this part

**M = Ti: x-ray amorphous**

- high  $E_{\text{form}}$  of solid solutions
- low E of Ar reflected from sputter target

**M = Zr: nanocomposite containing**

- $ZrB_xC_yN_{1-x-y}$  ( $x \geq 0.25$ )
- $ZrC_yN_{1-y}$
- amorphous phase (reminder: M content well below 50 at. %)
- HRTEM: the amorphous phase is around "nanoneedles"

*[M. Zhang et al., Acta Materialia 77, 212 (2014)]*

**M = Hf: nanocomposite containing**

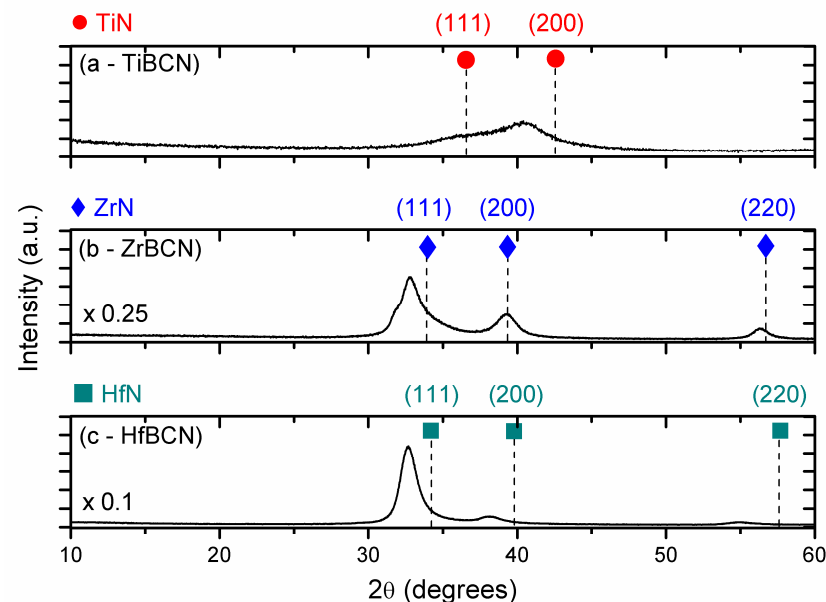
- $HfB_xC_yN_{1-x-y}$  (higher x compared to M = Zr)
- amorphous phase (reminder: M content well below 50 at. %)



## Two more remarks (i) On the preferred orientation

Observation: preferred orientation of MBCN solid solution is 111  
× preferred orientation of B-free Zr(C)N is 200

Explanation: lower diffusion rate on 111 surface (3 "backbonds")  
(part of) Growth of non-segregated solid solutions requires  
less diffusion  $\Rightarrow$  111 relatively more likely.

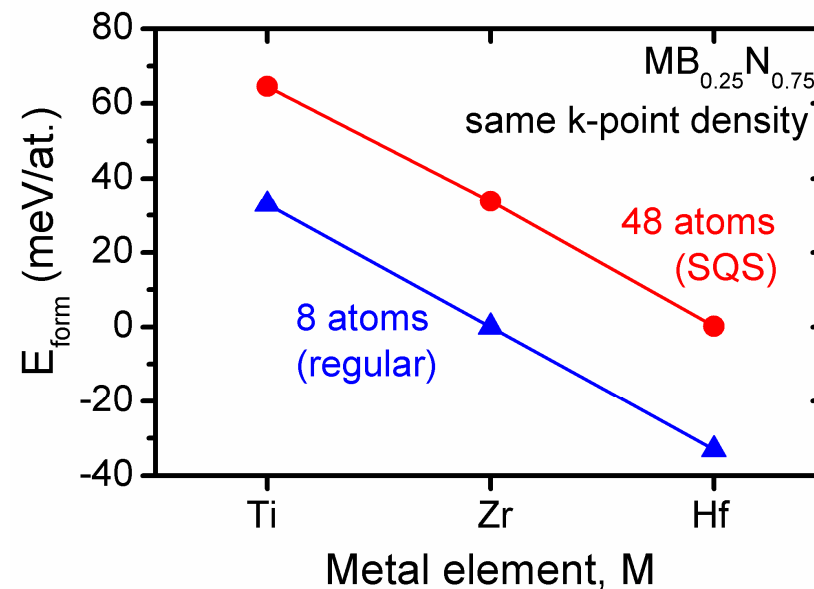


## Two more remarks (ii) On the distribution of B,C,N atoms

8 atoms ( $M_4BN_3$ )  $\Rightarrow$  regular distribution of atoms: lower  $E_{\text{form}}$

- thermodynamically (not kinetically) more preferred
- used in the rest of this presentation

48 atoms ( $M_{24}B_6N_{18}$ ), quasirandom SQS cell: higher  $E_{\text{form}}$

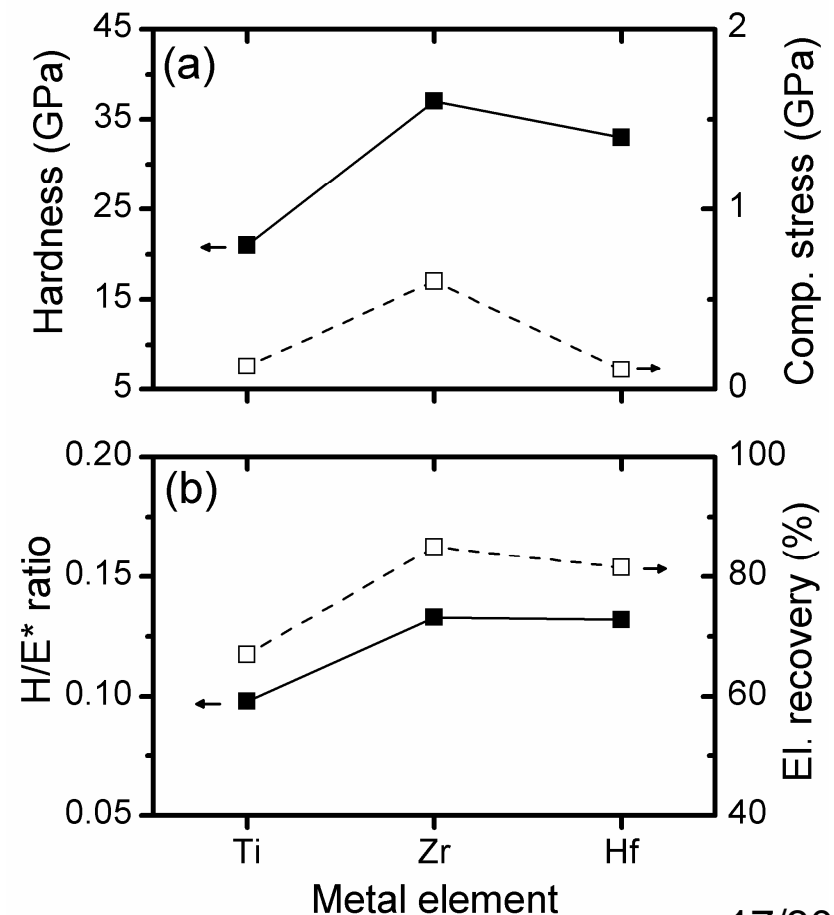


same trends of  $E_{\text{form}}$  along  $\text{Ti} \rightarrow \text{Zr} \rightarrow \text{Hf}$ , same lattice constants

## Effect of M choice on mechanical properties

Transition from amorphous TiBCN to nanocomposite ZrBCN and HfBCN improves

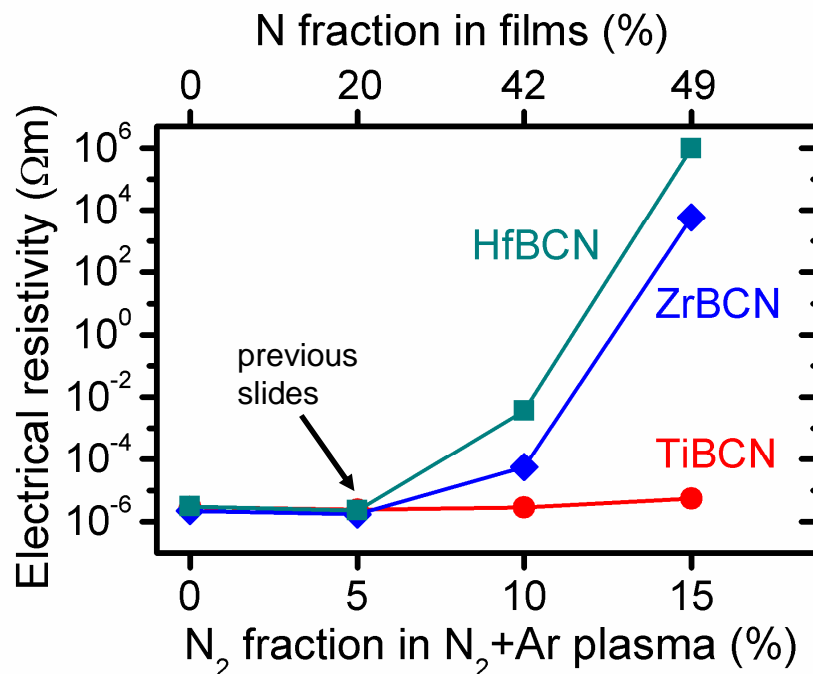
- hardness (21 → 33-37 GPa)
- el. recovery (67 → 82-85%)
- $H/E^*$  ratio (0.098 → 0.132-0.133)



## Effect of M choice on electrical resistivity

Varied N content ( $\Rightarrow$  leaving the  $M_{41}B_{30}C_8N_{20}$  composition)

- first impression:  $Ti \rightarrow Zr \rightarrow Hf$  enhances N incorporation
- RBS shows metal-independent N contents: any other (calculations-based) explanation of different resistivities?



15%  $N_2$  in  $N_2+Ar$

$M = Ti : \rho \sim 10^{-6} \Omega m$

$M = Zr : \rho \sim 10^3 \Omega m$

$M = Hf : \rho \sim 10^6 \Omega m$

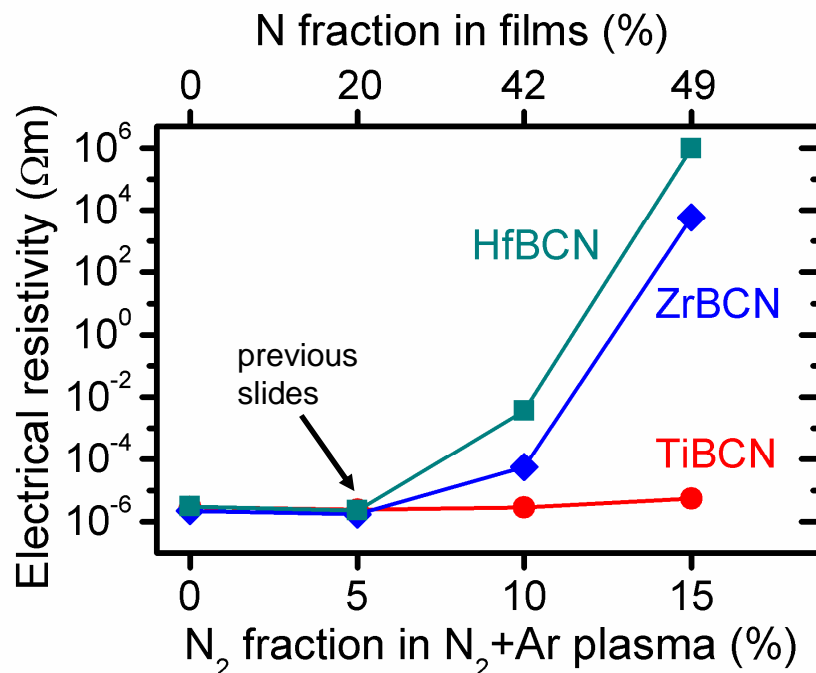
## Effect of M choice on electrical resistivity

Varied N content ( $\Rightarrow$  leaving the  $M_{41}B_{30}C_8N_{20}$  composition)

**M = Ti: homogenous M-containing conductive material**

**M = Zr: M segregated into conductive nanocrystals, separated by insulating a-BCN (BN: band gap  $\geq 5.2$  eV)**

**M = Hf: even lower  $E_{\text{form}}$  of nanocrystals  $\Rightarrow$  trend continues**



15%  $N_2$  in  $N_2+Ar$

**M = Ti :  $\rho \sim 10^{-6} \Omega m$**

**M = Zr :  $\rho \sim 10^3 \Omega m$**

**M = Hf :  $\rho \sim 10^6 \Omega m$**

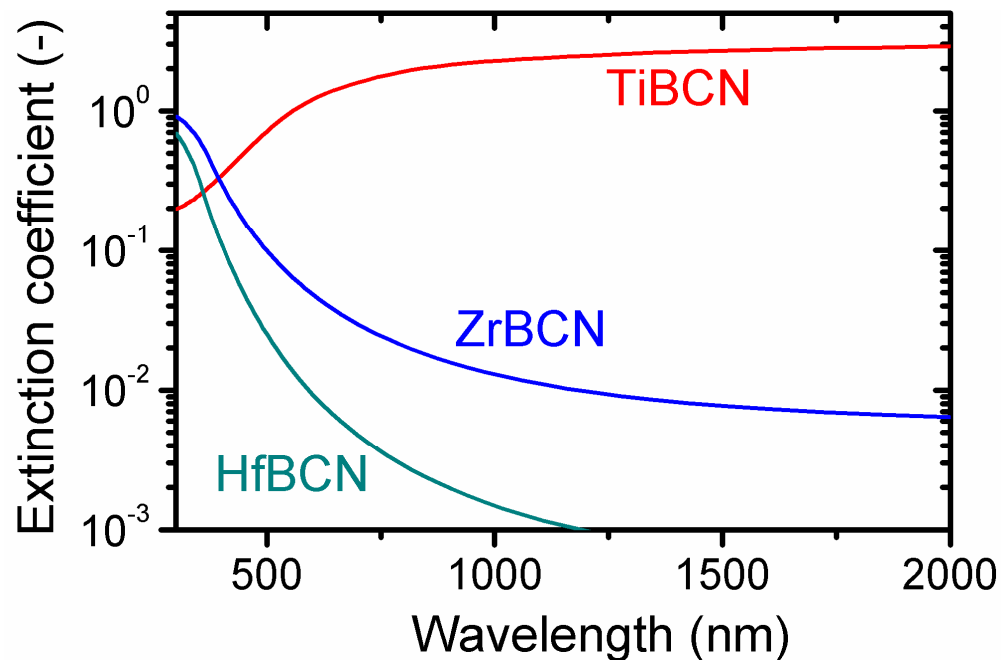
## Effect of M choice on optical transparency

Shown for N-rich compositions (15% N<sub>2</sub> in N<sub>2</sub>+Ar plasma)

M = Ti: homogenous M-containing opaque material

M = Zr: M segregated into opaque nanocrystals, separated by transparent a-BCN (BN: band gap  $\geq 5.2$  eV)

M = Hf: even lower  $E_{\text{form}}$  of nanocrystals  $\Rightarrow$  trend continues



15% N<sub>2</sub> in N<sub>2</sub>+Ar

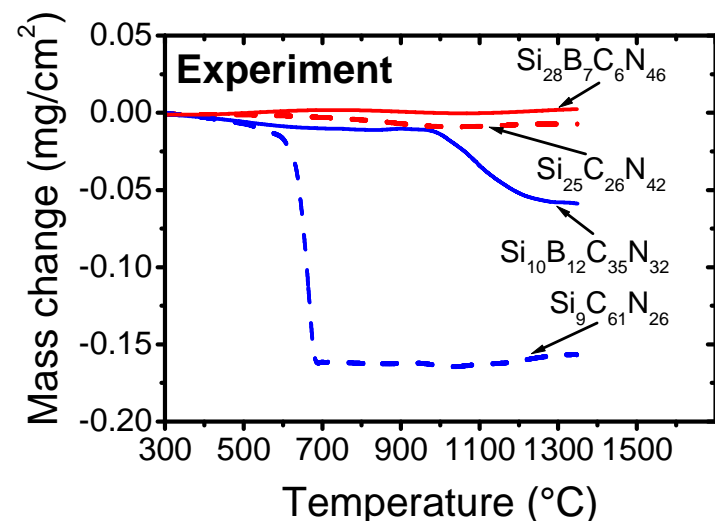
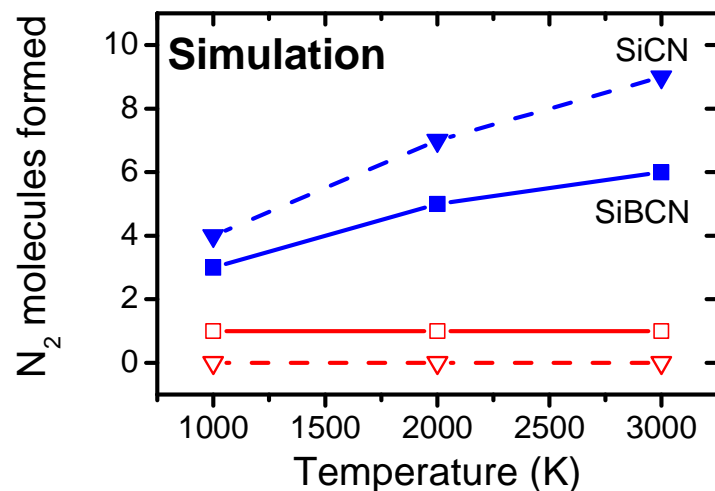
M = Ti :  $k_{550} = 0.98$

M = Zr :  $k_{550} = 0.06$

M = Hf :  $k_{550} = 0.014$

## Moving to oxidation resistance $\Rightarrow$ moving to MSiBCN

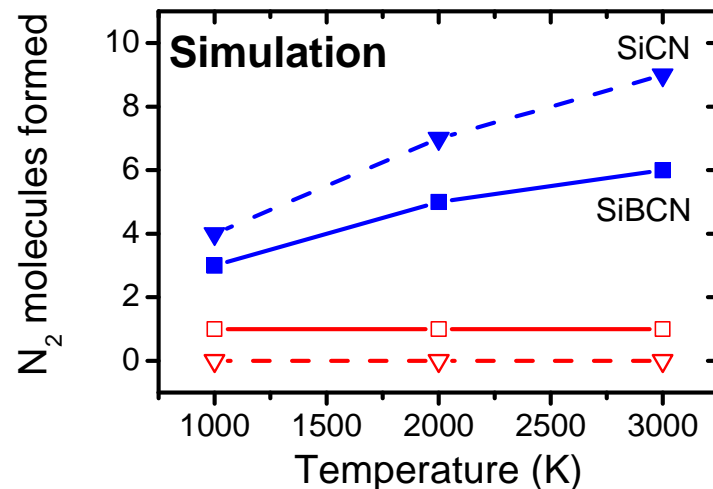
Thermal stability and oxidation resistance is improved by Si



- Thermal stability by MD simulations of N<sub>2</sub> formation  
 $\text{a-Si}_{39}\text{B}_{14}\text{C}_{11}\text{N}_{44}$ ,  $\text{a-Si}_{53}\text{C}_{11}\text{N}_{44}$ ,  
 $\text{a-Si}_{11}\text{B}_{14}\text{C}_{39}\text{N}_{44}$ ,  $\text{a-Si}_{11}\text{C}_{53}\text{N}_{44}$
- Decomposition reactions  
 $\text{Si}_3\text{N}_4 + 3\text{C} \Rightarrow 3\text{SiC} + 2\text{N}_2$   
and  $\text{Si}_3\text{N}_4 \Rightarrow 3\text{Si} + 2\text{N}_2$   
 $\Rightarrow$  mass loss due to N<sub>2</sub>
- Less N<sub>2</sub> molecules formed at  
(1) higher **Si/C** ratio and  
(2) **B** addition

## Moving to oxidation resistance $\Rightarrow$ moving to MSiBCN

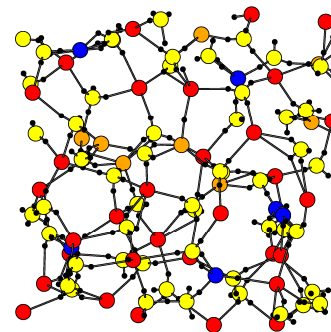
Thermal stability and oxidation resistance is improved by Si



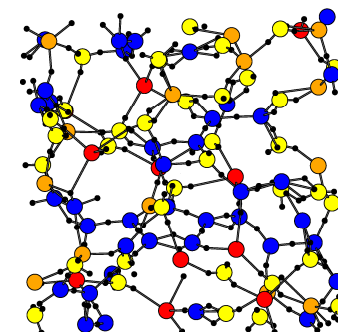
- Thermal stability by MD simulations of N<sub>2</sub> formation

**a-Si<sub>39</sub>B<sub>14</sub>C<sub>11</sub>N<sub>44</sub>, a-Si<sub>53</sub>C<sub>11</sub>N<sub>44</sub>,**  
**a-Si<sub>11</sub>B<sub>14</sub>C<sub>39</sub>N<sub>44</sub>, a-Si<sub>11</sub>C<sub>53</sub>N<sub>44</sub>**

Si-rich



C-rich



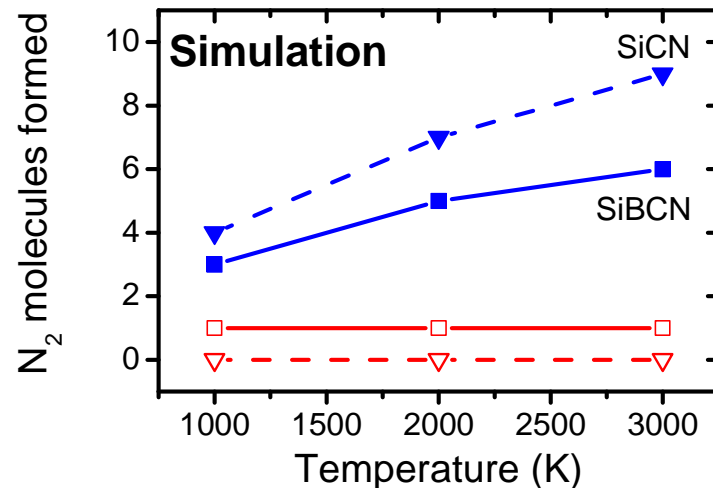
Si: ●, B: ●, C: ●, N: ●,

2 valence electrons: —●—

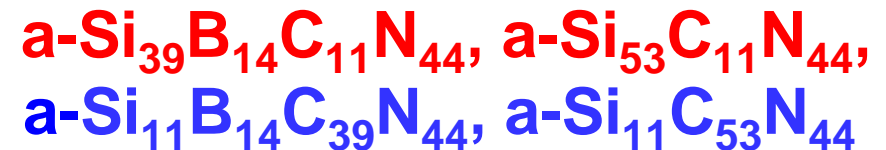


## Moving to oxidation resistance $\Rightarrow$ moving to MSiBCN

Thermal stability and oxidation resistance is improved by Si



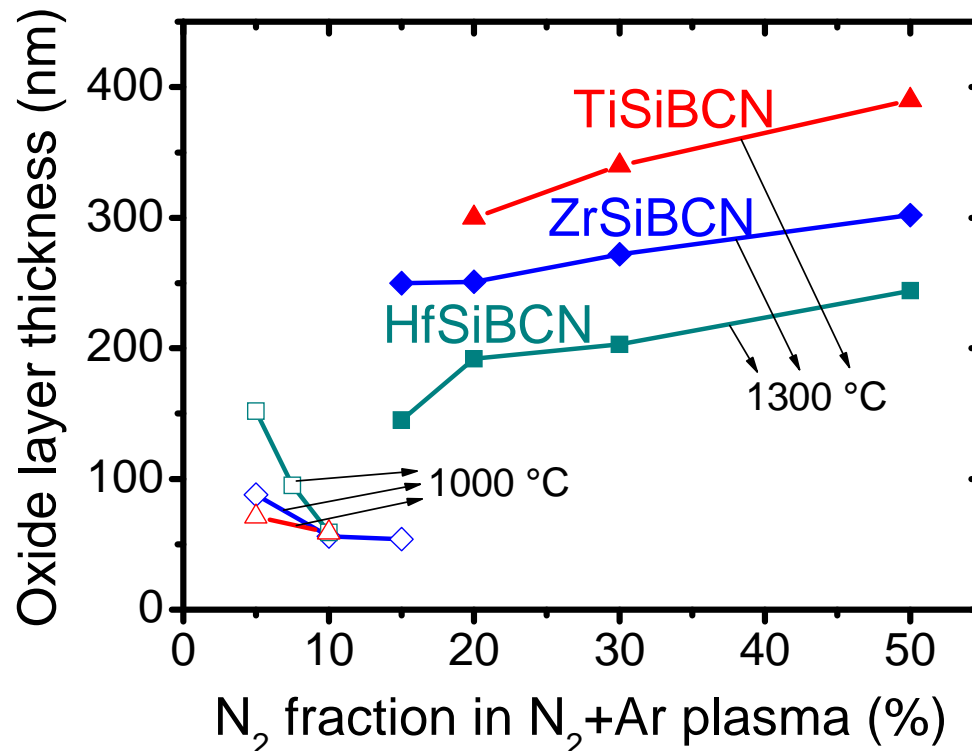
- Thermal stability by MD simulations of N<sub>2</sub> formation



$\Rightarrow$  moving from **MBCN** [  $\text{M}_{45}(\text{B}_4\text{C})_{55}$  sputter target ]  
 to **MSiBCN** [  $\text{M}_{15}(\text{B}_4\text{C})_{65}\text{Si}_{20}$  sputter target ]

## Effect of M choice on oxidation resistance (experiment)

- $M_{15}(B_4C)_{65}Si_{20}$  sputter target
- **Oxide layer thickness** (measured by spectroscopic ellipsometry) after annealing in air up to 1000 and 1300 °C



**N-poor** ( $\Rightarrow$  higher M content) at 1000 °C

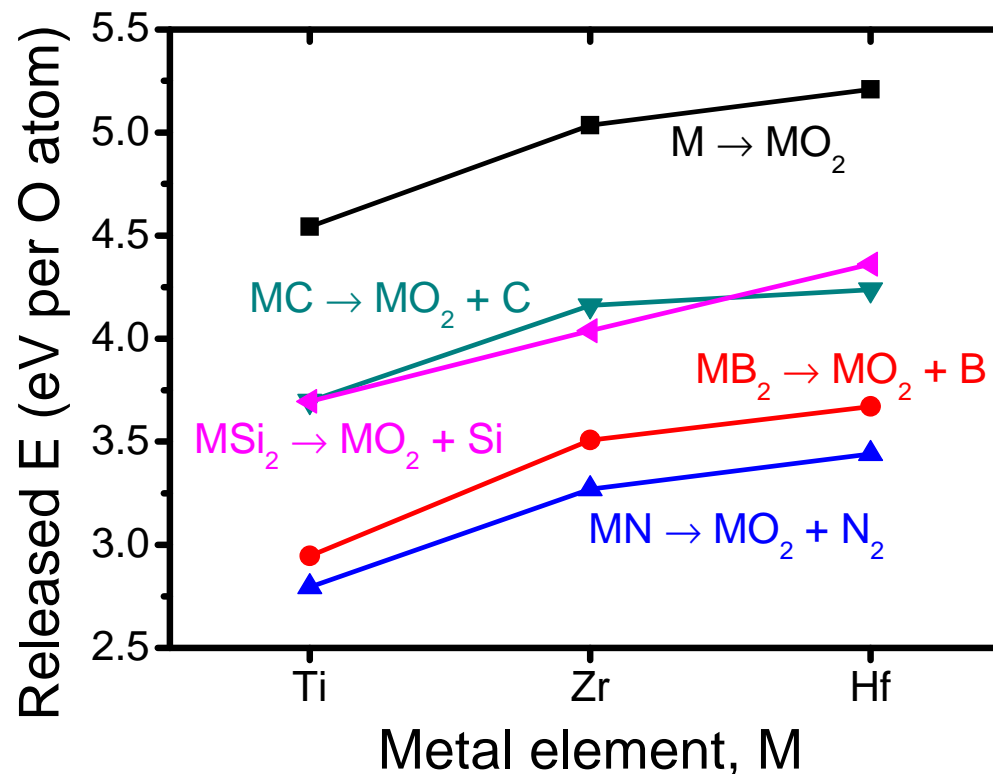
best Ti  $\rightarrow$  Zr  $\rightarrow$  worst Hf

**N-rich** ( $\Rightarrow$  lower M content) at 1300 °C

worst Ti  $\rightarrow$  Zr  $\rightarrow$  best Hf

**Effect of M choice on oxidation resistance:**  
Calculations relevant for M-rich crystalline compositions  
( $E_{\text{form}}$  of crystals and molecules)

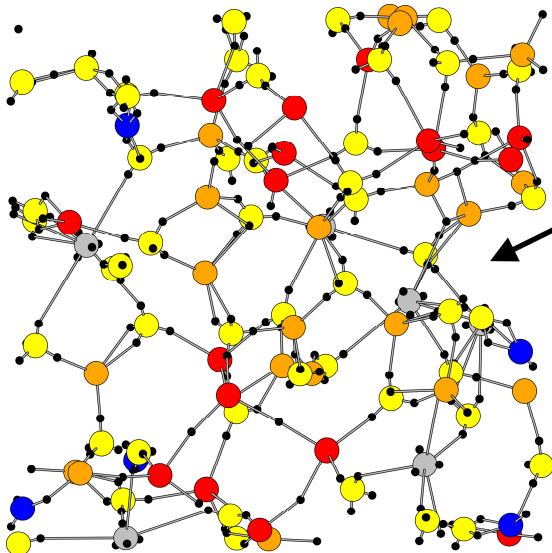
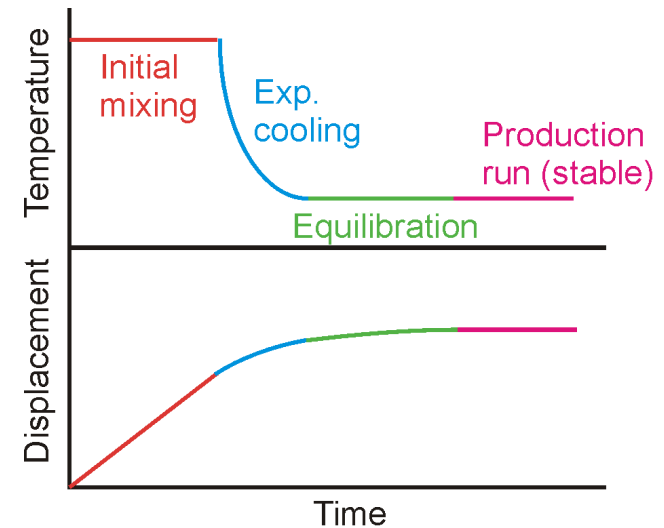
**Energy released during oxidation increases  
from M = Ti through Zr to Hf**



## Effect of M choice on oxidation resistance (calculation)

Calculations relevant for M-poor (N-rich) compositions  
(bonding preferences in amorphous networks)

**Liquid-quench algorithm** captures material formation conditions arising from rapid cooling of the localized melt around sites of ion impact



example shown for  $\text{Hf}_6\text{Si}_{17}\text{B}_{22}\text{C}_5\text{N}_{50}$

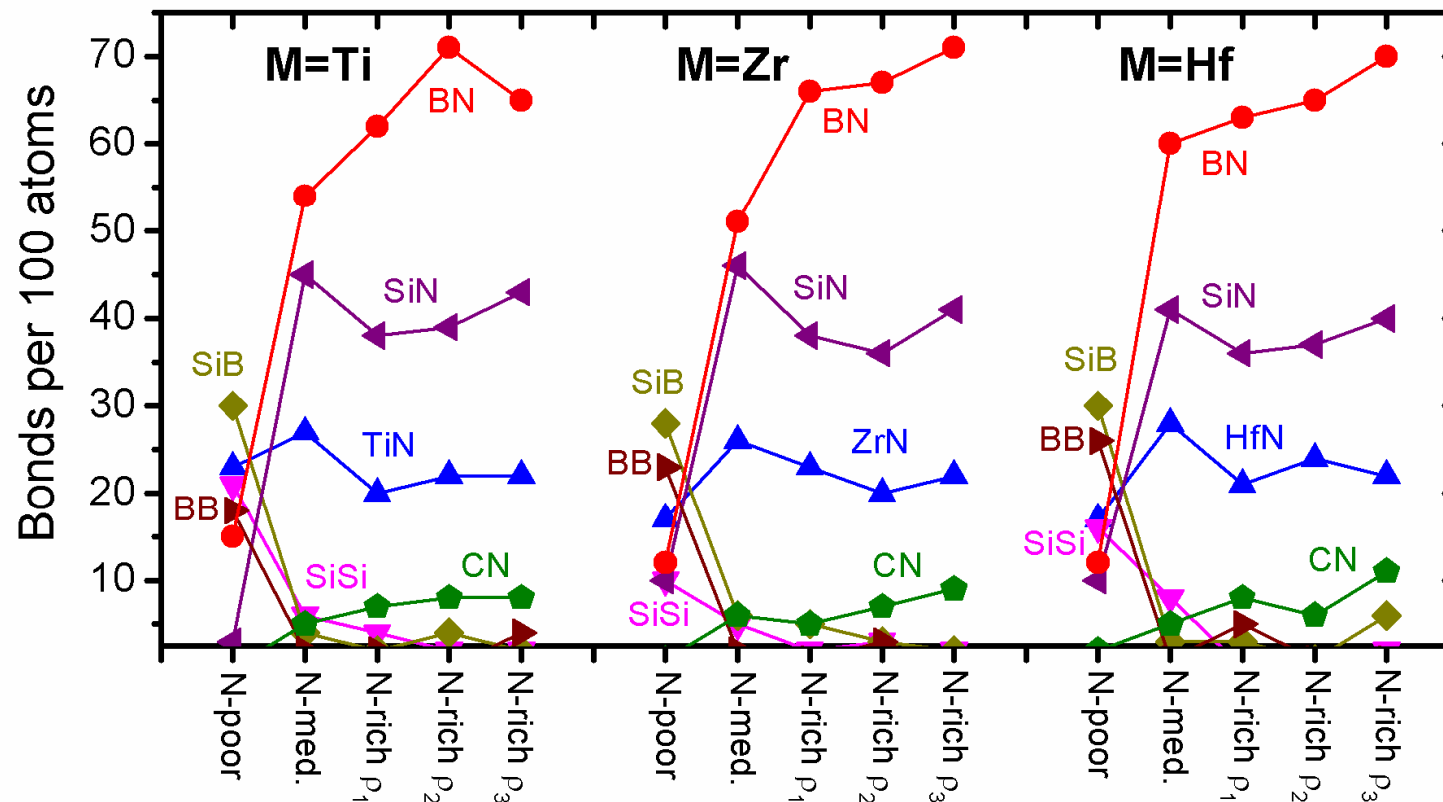
Si: ●, B: ●, C: ●, N: ●, Hf: ●

2 valence electrons: —●—

## Effect of M choice on oxidation resistance (calculation)

Calculations relevant for M-poor (N-rich) compositions  
(bonding preferences in amorphous networks)

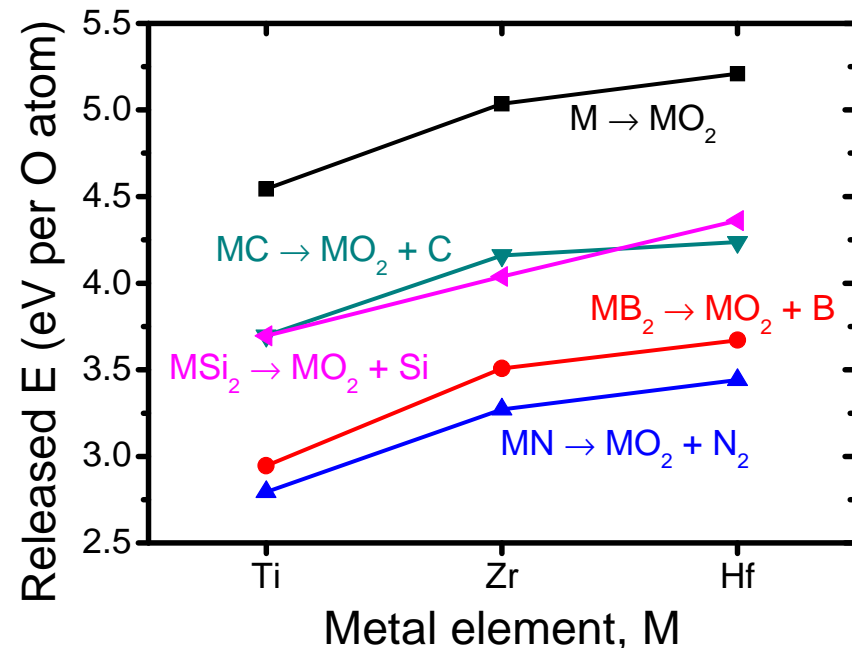
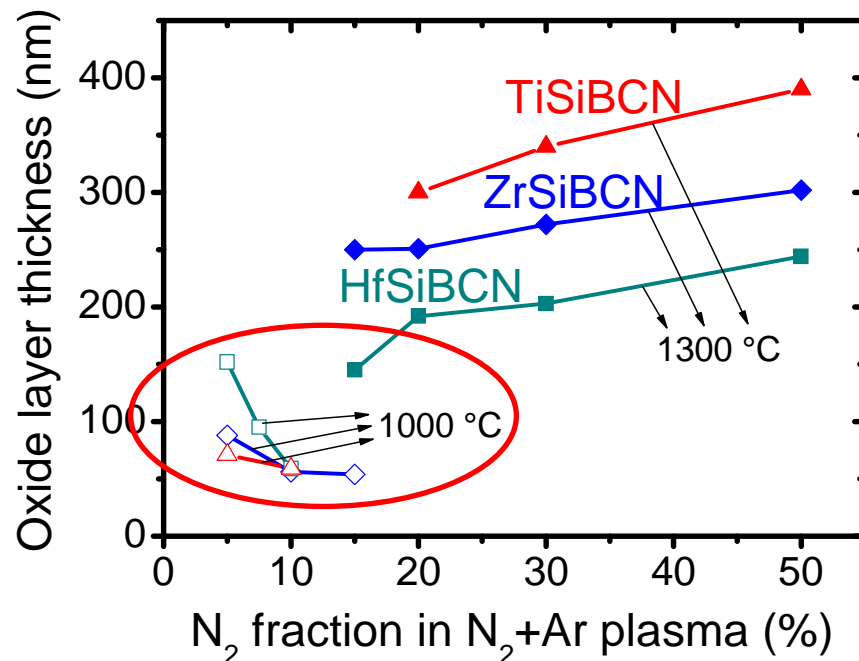
3 compositions ( $M_{16}Si_{27}B_{36}C_9N_{12}$ ,  $M_6Si_{17}B_{22}C_5N_{50}$ ,  $M_5Si_{13}B_{26}C_6N_{50}$ ),  
3 densities for the last composition ... but **no real differences**



## Effect of M choice on oxidation resistance

explanation for M-rich ( $\Leftrightarrow$  N-poor) MSiBCN

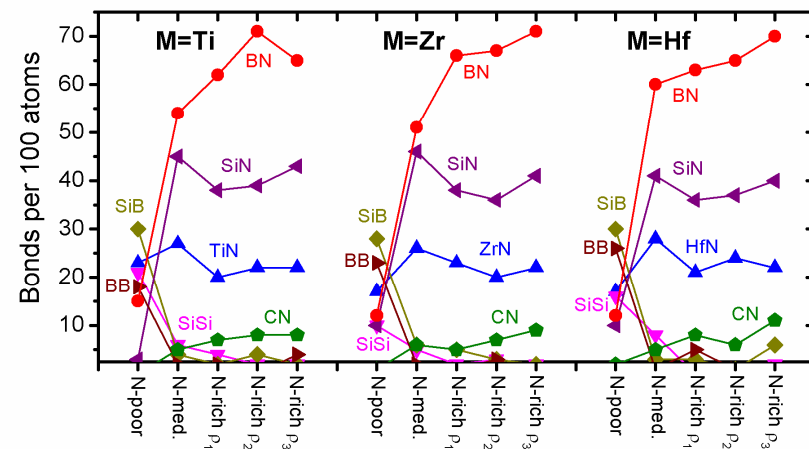
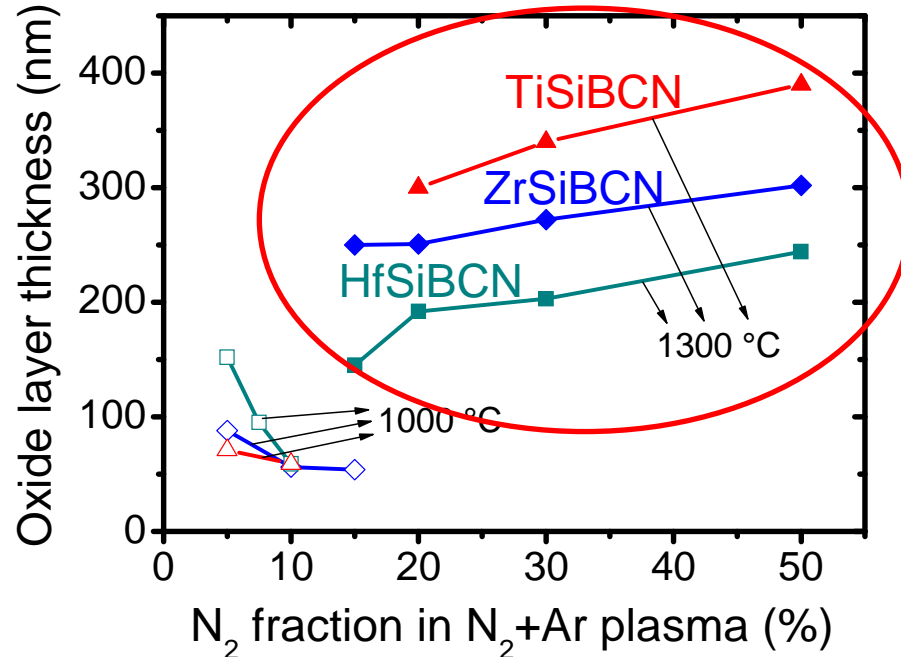
- decreasing oxidation resistance from **Ti** through **Zr** to **Hf**
- explained by **calculated energies of M-based compounds**  
(**Ti**→**Zr**→**Hf**  $\Rightarrow$  higher driving force towards oxidation)



## Effect of M choice on oxidation resistance

explanation for M-poor ( $\Leftrightarrow$  N-rich) amorphous MSiBCN

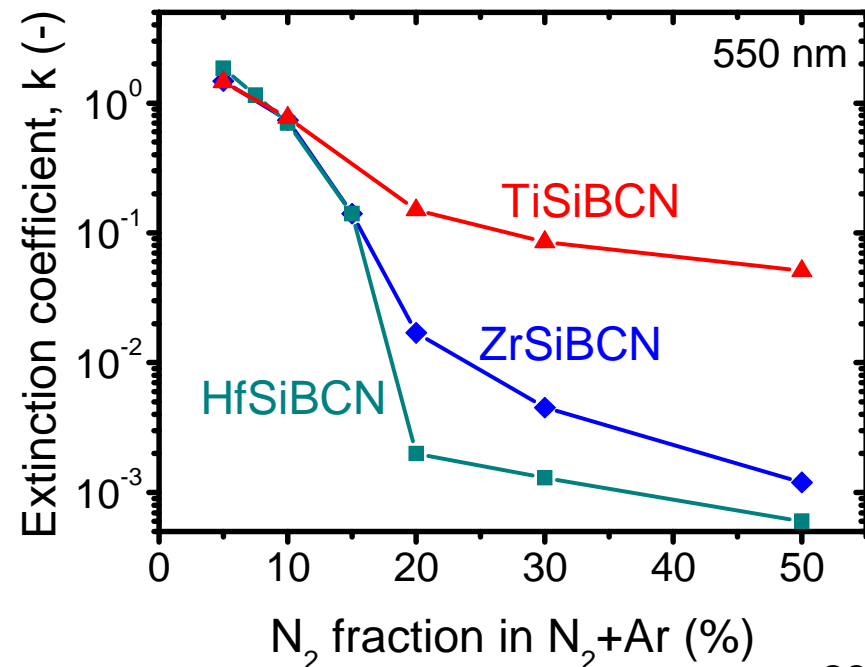
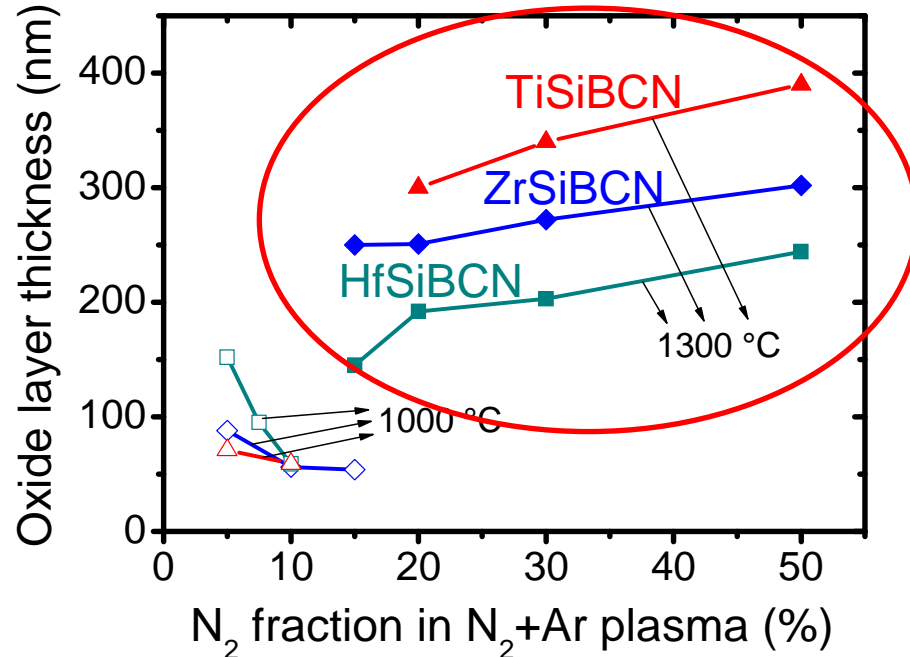
- increasing oxidation resistance from **Ti** through **Zr** to **Hf**
- not explained by calculated bonding statistics
- above: **Ti/Zr/Hf**-based MBCN are not "equally amorphous"
- here: **Ti/Zr/Hf**-based MSiBCN are not equally amorphous either



## Effect of M choice on oxidation resistance

explanation for M-poor ( $\Leftrightarrow$  N-rich) amorphous MSiBCN

- increasing oxidation resistance from **Ti** through **Zr** to **Hf**
- above: **Ti**→**Zr**→**Hf** decreases  $k$  of MBCN (calculated  $E_{\text{form}}$  !)
- here: **Ti**→**Zr**→**Hf** decreases  $k$  of MSiBCN as well  
 $\Leftrightarrow$  (once again) slight **segregation** or slightly higher N content







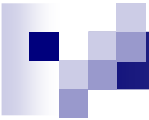
## Conclusions 1/2 - fundamental differences

**Experiment:** Ti→Zr→Hf leads to

- Increasing  $E$  of reflected Ar  
(suppressed by varied pressure)
- Possibly easier N incorporation  
(not measurable directly, but can explain better transparency)

**Calculations:** Ti→Zr→Hf leads to

- Decreasing  $E_{\text{form}}$  of cubic (MN-like) solid solution crystals
- Increasing energy relieved after oxidation of M-based crystals
- Same bonding preferences in amorphous networks



## Conclusions 2/2 - consequences

**Low (~20 at. %) N content:**  $\text{Ti} \rightarrow \text{Zr} \rightarrow \text{Hf}$  leads to

- Transition from  $\text{a-TiBCN}$  through nanocomposite  $\text{ZrB}_x\text{C}_y\text{N}_{1-x-y}/\text{ZrC}_y\text{N}_{1-y}/\text{a-(Zr)BCN}$  to  $\text{HfB}_x\text{C}_y\text{N}_{1-x-y}/\text{a-BCN}$
- Consequently enhanced hardness, elastic recovery,  $H/E^*$
- Worse oxidation resistance (at 1000 °C) of MSiBCN

**High (~50 at. %) N content:**  $\text{Ti} \rightarrow \text{Zr} \rightarrow \text{Hf}$  leads to

- Increasing electrical resistivity
- Decreasing extinction coefficient (better transparency)
  - of M-rich MBCN
  - of M-poor MSiBCN
- Better oxidation resistance (at 1300 °C) of MSiBCN